MYELIN MEMBRANE STRUCTURE AS REVEALED BY X-RAY DIFFRACTION

DAVID HARKER

From the Center for Crystallographic Research, Roswell Park Memorial Institute, Buffalo, New York 14203

ABSTRACT The present work consists of a new interpretation of the data presented in the article entitled "X-Ray Diffraction of Myelin Membrane. II" by C. K. Akers and D. F. Parsons (1970, *Biophys. J.* **10**:116). It will be shown that the projection of the electron density onto the normal to the myelin multilayer derived by these authors is no more consistent with their data than another electron density function, or, perhaps, its negative. (A density function and its negative are related as follows: one of them is a certain density distribution, the other is the same function subtracted from a constant uniform density. Two density functions so related produce identical diffracted intensities.) The Fourier series for the projection of the electron density onto the normal to the myelin multilayer has coefficients $\pm[hI(h)]^{1/2}$ where $I(h)$ are the intensities of the five orders of reflection; data from which these can be estimated are presented by Akers and Parsons. The sequence of signs found here is $+ - - + +$ for the positive density (or $- + + - -$ for the negative one). Quantitative agreement exists between the five X-ray diffraction data of Akers and Parsons and the same intensities calculated from the new model of the myelin structure described here. In this model the myelin double layer, 171 A thick, consists of a central lipid layer 72.4 A thick covered on both surfaces by protein layers 6.9 A thick; these protein layers are covered, in turn, by other lipid layers 42.4 A thick. Minor modifications of this model will no doubt be required to produce agreement between the observed and calculated intensities of the higher order reflections.

INTRODUCTION

C. K. Akers and D. F. Parsons describe in their article in the *Biophysical Journal* (1) their methods for preparing X-ray diffraction patterns from frog sciatic nerve, and show diagrams containing information about these diffraction patterns; they have graciously permitted me to use the original prints from which these diagrams were made. The experimental technique and methodology appear excellent, and it would seem that the data to be derived from these diagrams are quite reliable (just how reliable will be discussed below). It is the interpretation of these data that is under discussion here.

The computation of the electron density function from the X-ray scattering pattern involves assigning phases to the scattering amplitudes derived from the intensities.

Inasmuch as these phases cannot be observed directly, various indirect methods of obtaining these phases have been applied to the myelin X-ray diffraction data by a number of authors. (See Akers and Parsons for references.) In Akers and Parsons, the method of introducing a small amount of material containing atoms of high atomic number is used; this is called "heavy atom labeling." The diffracted intensities change progressively as the amount of labeling is increased, if the heavy atoms attach themselves to the same kinds of position in each repeating unit of the structure. The positions of the heavy atoms can be found from these intensity changes by standard methods used in X-ray crystallography; the phases of the scattering amplitudes then follow from a knowledge of these positions. Akers and Parsons arrived at heavy atom positions, phases, and a structure for myelin which is different from the structure obtained by usual methods of analysis. The usual methods will be applied in the following paragraphs, and the resulting structure described.

ELECTRON DENSITY FUNCTION

The electron microscope work on the myelin sheath of nerves indicates that it can be considered as formed from a single sheet of membrane by folding it once back onto itself and then wrapping this double layer around the nerve fiber several hundred times, thus forming the outer part of a circular cylinder. It is, therefore, a structure which is periodic in the radial direction, with a period of the thickness of one double layer, 171 A. There is a center of inversion relating the projection of the electron density onto the normal of each single layer with the same kind of projection of each of its neighboring single layers; they can be described as lying face-to-face and back-to-back. The reflection of X-rays from the surface of such a multilayer occurs only at the glancing angles allowed by the Bragg law of X-ray diffraction: $h\lambda = 2d\sin\theta$. At very small glancing angles θ, this equation can be written $h\lambda = 2d\theta$. Here h is the "order" of the reflection, λ the wavelength of the X-rays, and d the length of one period. The intensities enter the computation of the projection of the electron density onto the normal to the multilayer, $\rho(l)$, according to the equation:

$$\rho(l) = \frac{1}{d}\sum_{h=0}^{\infty} s(h)[hI(h)]^{1/2}\cos 2\pi hl. \qquad (1)$$

Here l is the distance along the normal in units of the period d, $I(h)$ is the absolute intensity of the hth order of reflection, and $s(h)$ is the sign appropriate to that order. The quantity $[hI(h)]^{1/2}$ (with the square root taken positive) is the magnitude of the scattering amplitude $|F(h)|$; the sign $s(h)$ of each such coefficient is all the phase information required in the case of a centrosymmetric repeat unit; thus, $F(h) = s(h)\,|F(h)| = s(h)\,[hI(h)]^{1/2}$. Clearly, the quantities required to compute $\rho(l)$ are all obtained directly from the diffraction pattern reflected from the myelin multilayer, except the signs $s(h)$. Five orders of reflection ($h = 1, 2, 4, 3, 5$) have been observed to be important enough to affect markedly the Fourier series (1) for $\rho(l)$.

Thus, there would appear to be $2^5 = 32$ different possible structures $\rho(l)$ compatible with the diffraction pattern of untreated myelin; however, each structure responds to two sequences of signs, depending on which of the two different centers of inversion is used as the origin of coordinates, and the negative of each structure corresponds to the reverse set of signs. Consequently, there are only $32/4 = 8$ fundamentally different structures for myelin to be derived from the five quantitatively observed diffraction maxima.

The Patterson function, a Fourier series with the coefficients $hI(h)$,

$$P(l) = \frac{1}{d} \sum_{h=0}^{\infty} hI(h) \cos 2\pi hl, \qquad (2)$$

is independent of the signs $s(h)$; it represents the number of interelectronic distances of length l. Every Patterson function has an extremely large peak at the origin ($l = 0$) corresponding to the fact that every electron in the structure is at zero distance from itself. Peaks at other values of l indicate the presence of important interelectronic, and therefore interatomic, distances in the structure. The various possible density functions $\rho(l)$ are all consistent with the function $P(l)$, no matter what choices of signs $s(h)$ are made.

HEAVY ATOM POSITIONS AND CORRESPONDING PHASES

Fig. 2 of Akers and Parsons presents the intensities of the X-ray diffraction maxima for unlabeled myelin, and for myelin exposed for various times to the vapor from OsO_4 solution. A heavy, sloping line indicates the trend of the intensity of each maximum as the time of exposure increases. (See Akers and Parsons for the experimental details.) Measurements of the ordinates of these heavy lines drawn on the original prints of Fig. 2, in millimeters, gave the numbers in Table I for untreated myelin, "$I(h)$, 0 min," and for myelin exposed to OsO_4 vapor for 10 min, "$I(h)$, 10 min."

As the time of exposure of the myelin to the OsO_4 vapor increased, the values of $|F(h)|$ of all the orders increased, but by different amounts (see Table I, rows 3 and

TABLE I

DIFFRACTED X-RAY INTENSITIES FROM MYELIN AND FROM MYELIN TREATED WITH OsO_4 FOR 10 MIN, AND VALUES OF SOME DERIVED QUANTITIES

h	1	2	3	4	5
$I(h)$, 0 min	0.9	36.6	4.5	26.2	2.1
$I(h)$, 10 min	4.0	82.5	20.1	35.9	15.7
$\lvert F_0(h) \rvert = [hI(h)]^{1/2}$, 0 min	0.9	8.6	3.7	10.2	3.2
$\lvert F_{10}(h) \rvert = [hI(h)]^{1/2}$, 10 min	2.0	12.9	7.8	12.0	8.9
$\lvert F_{10} \rvert - \lvert F_0 \rvert = \Delta \lvert F \rvert$	1.1	4.3	4.1	1.8	5.7
$5.88\Delta \lvert F \rvert$	6	25	24	11	34
$(5.88\Delta \lvert F \rvert)^2$	36	625	576	121	1156

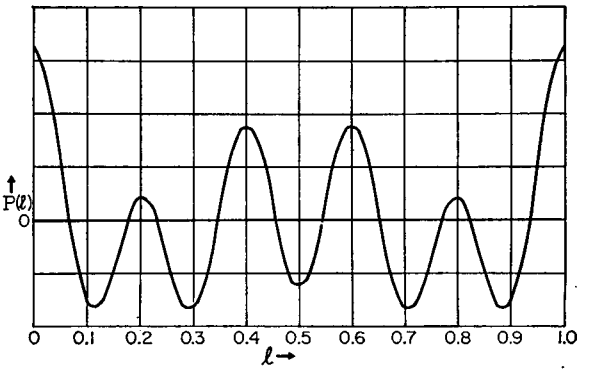

FIGURE 1 Five-term Fourier series for the Patterson function of the osmium labeling of myelin. Coefficients are the squares of the differences between the magnitudes of the quantities $[hI(h)]^{1/2}$ for the untreated and osmium-labeled myelin. (The vertical scale is arbitrary.)

4). This shows that the signs of the contributions of the Os atom structure to the amplitudes must be the same as those of the amplitudes of the myelin structure itself. Subtracting row 3 from row 4 we thus obtain the magnitudes $\Delta \mid F(h) \mid$ of the amplitudes of the Os structure, shown in row 5. These were "normalized" by multiplying each term by

$$100\left[\sum_{h=1}^{5} \Delta \mid F(h) \mid\right]^{-1} = 5.88,$$

to give the numbers in row 6. The squares of these last numbers appear in row 7; they are proportional to the coefficients used in computing the Patterson function (i.e., in equation 2) in order to find the distribution of the Os–Os distances. A graph of this function appears in Fig. 1.

Fig. 1 shows the expected origin peak corresponding to the osmium self-distances, a strong peak at $l = 0.40$ corresponding to an Os–Os projected distance of 68.4 A, and a minor peak at 0.20 which might correspond to an Os–Os distance of 34.2 A, but can reasonably be assumed to be a ripple caused by cutting off the Fourier series after only the fifth term. There being, therefore, only one important nonzero Os–Os distance and a center of inversion being present, there must be, in the projected structure of osmium-treated myelin, groups of osmium atoms at about $l = \pm 0.20$. Their contribution to the amplitudes whose magnitudes appear in row 6 of Table I will therefore be proportioned to

$$\Delta F(h) = 2f(h)\cos 2\pi hl, \tag{3}$$

where h runs from 1 to 5, l is near 0.20, and $f(h)$ is the scattering power of a single osmium layer.

The widths at half-height of the peaks in the Patterson function of Fig. 1 can be no

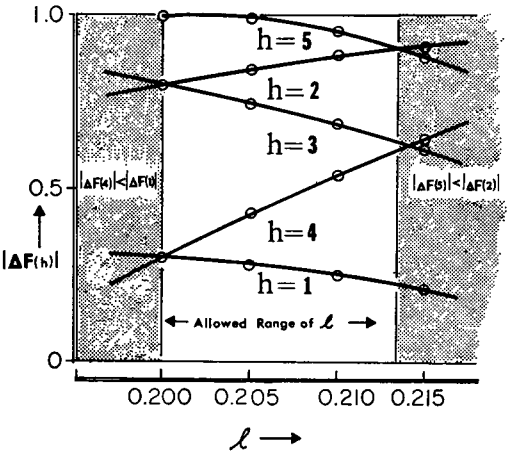

FIGURE 2 Limitation of the parameter l of the osmium-labeled lamella in osmium-treated myelin. (The vertical scale is arbitrary).

smaller than about $d/10$, since the shortest wavelength of the Fourier terms is $d/5$, i.e., about 17 A; this is the maximum spread that a single osmium layer can have, but any smaller value is possible. If the distribution of osmium atoms in a single layer is assumed to be gaussian, then the behavior of $f(h)$ is also gaussian and can be represented by

$$f(h) = f_0 e^{-Ah^2}, \tag{4}$$

where f_0 is the scattering power of a hypothetical osmium layer for which all the atoms project onto a single point of the layer normal, and A is another constant which specifies the spread of the osmium atoms' distribution. It is customary in finding a structure to assume initially that $A = 0$, then to vary l in equation 3 until an approximate proportionality between $|\Delta F(h)|$ as calculated and as observed is obtained, and then to vary all three parameters l, f_0, and A to achieve the best possible agreement.

We have $|\Delta F(5)| > \Delta F(2)| > |\Delta F(3)| > |\Delta F(4)| > |\Delta F(1)|$ and $l \cong 0.2$. The fact that $|\Delta F(5)|$ is so large indicates that A is quite small, so that $A = 0$ can be used as a practical starting artifice. Furthermore, at $l \lessapprox 0.200$, $|\Delta F(4)| \cong |\Delta F(1)|$ by equation 3, and this is contrary to observation; therefore $l > 0.200$. If $l > 0.214$, $|\Delta F(5)| \leqq |\Delta F(2)|$ by the same equation; hence $l < 0.214$. The allowed range of l is thus $0.200 \leqq l < 0.214$. All this is illustrated in Fig. 2. Inasmuch as the inequalities defining this range depend on the condition that the $|\Delta F|$ of a high order reflection is larger than that of one of lower order, a value of A in equation 4 larger than zero can only narrow the acceptable range of l still further. With $f_0 = 30.7$, $A = 0.000$, and $l = 0.202$, satisfactory proportionality is obtained between the observed $|\Delta F(h)|$'s (Table I, row 5 or 6) and the ones computed using equation 3. (Of course,

$A = 0.000$ cannot be correct, since this would mean that the osmium atoms project onto the layer normal as points. A must be small, however, and the osmium layers are, therefore, quite thin.) For any l in the allowed range the values of the quantities $s(h)$ in equation 1 are, in order of increasing h, $+--++$. These are the signs of the osmium contributions to the $F(h)$'s of the labeled myelin, and are also those of the unlabeled myelin, since these must be the same, as noted previously. (If the origin is taken at $l = 0.500$, then the signs of the $F(h)$'s of odd order must all be changed, if equation 1 is to describe the same electron density; the sequence of signs would then be $--+-+$.)

INTENSITY DATA FOR UNLABELED MYELIN

On the original plates of Figs. 2, 4, and 5 of Akers and Parsons are plotted the intensities of the first five orders of X-ray diffraction from unlabeled myelin. On Figs. 2 and 4, these data are plotted on the ordinates for zero labeling time; on Fig. 5, they are plotted on the ordinates for zero concentration. On each of these ordinates appears a dark band indicating the range of the experimentally observed intensities for that particular specimen of myelin. It can be assumed that the center point of each dark band is the best estimate for the ordinate representing the corresponding intensity. The height in millimeters of this point above the base line was measured for every order on the original print of each figure; this number was then multiplied by the order of the reflection, to correct for the Lorentz and polarization factors, and the square root of the result computed, thus providing numbers proportional to the magnitudes of the structure amplitudes $|F(h)|$. The five $|F(h)|$'s derived from each figure were then normalized, i.e., multiplied by a factor chosen to make their sum equal to 100. The resulting numbers are shown in Table II. (The data in Table I, row 3, are not exactly proportional to those in Table II, row 1, because of the slightly different method of measuring the intensities.)

TABLE II

MAGNITUDES OF THE STRUCTURE AMPLITUDES OF THE X-RAY DIFFRACTION MAXIMA OF UNTREATED MYELIN*

Order	$h = 1$	$h = 2$	$h = 3$	$h = 4$	$h = 5$
Fig. 2	3.6	32.1	13.6	36.0	14.7
Fig. 4	4.0	35.2	15.2	31.9	13.7
Fig. 5	3.6	32.4	16.3	31.0	16.7
$\sigma(\|F(h)\|)$	0.53	2.04	1.53	1.69	1.60
Mean $\|F(h)\|$ obs	3.7	33.2	15.0	33.0	15.0
$\|F(h)\|$ calc	4.2	35.3	11.6	32.6	16.4
$S(h)$	+	−	−	+	+
| Mean $\|F(h)\|$ obs − $\|F(h)\|$ calc |	0.5	2.1	3.4	0.4	1.4

* Computed from Figs. 2, 4, and 5 of Akers and Parsons and normalized to make $\sum |F(h)| = 100$. Some derived numbers are also included. For explanations, see the text.

The quality of these experimental data can be estimated by computing a value of $R(m, n)$ for each pair of figures,

$$R(m,n) = \frac{\sum | \, | F(h)m | - | F(h)n | \, |}{\frac{1}{2}\sum (| F(h)m | + | F(h)n |)},$$

where m and n refer to the figure numbers, and the summations are taken over all five orders h. The value of the denominator is always 100, because of the way the $| F(h) |$'s are normalized. The following values are obtained in this way: $R(2, 4) = 0.112$, $R(2, 5) = 0.106$, $R(4, 5) = 0.099$; the average of these three, $\bar{R} = 0.106$, is a measure of the reproducibility of the experimental determination of a set of five $| F(h) |$ values from different specimens of myelin, using the techniques of Akers and Parsons.

Another measure of the precision of a set of measurements is the root mean square deviation from the mean, $\sigma(x) = [\overline{x^2} - \bar{x}^2]^{1/2}$. If it is assumed that three identical specimens of myelin were used in the experiments which provided the data for Figs. 2, 4, and 5, then the differences among the $| F(h) |$'s in the three experiments are entirely due to the measuring technique, and it is appropriate to compute $\sigma[| F(h) |]$ for each h; the results appear on a row of Table II. The values of $s(h)$ in Table II are those obtained from the OsO_4 labeling experiment just described.

ELECTRON DENSITY FUNCTION OF UNLABELED MYELIN

Carrying out the computation of $\rho(l)$ according to equation 1 using the sign sequence $+--++$, the projection of the electron density of unlabeled myelin upon the normal to the multilayer is obtained; this is shown in Fig. 3. C. R. Worthington and A. E. Blaurock (2) have proposed that the sign sequence $-+--$ is to be applied to the first five $F(h)$'s of undyed myelin. They arrived at this result, which corresponds to my structure taken as negative, by following the changes in the intensities of the various orders of the X-ray diffraction pattern as the myelin was allowed to swell in sucrose solutions. Worthington and Blaurock made the assumption that the average electron density of the myelin double layer itself was less than that of the interstitial liquid medium which entered between neighboring myelin double layers as the swelling proceeded; this led them to an electron density which is qualitatively equivalent to mine subtracted from the constant density of the swelling medium. Worthington[1] has written me that the choice between the Worthington and Blaurock structure and mine is "not that definite." If he and Blaurock had assumed the average myelin density to be greater than that of the swelling medium, my results would have agreed completely with theirs.

The Patterson function for the osmium atom structure, Fig. 1, could have been

[1] Worthington, C. R. 1970. Private communication.

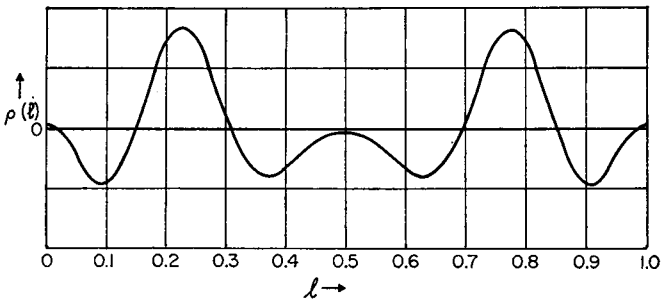

FIGURE 3 The sum of the first five terms of the Fourier series for the projection of the electron density of untreated myelin onto the normal to the multilayer. (The vertical scale is arbitrary.)

interpreted to indicate a perfectly uniform labeling of the complete double myelin layer, except for the regions close to $l = +0.202$ and -0.202 where the labeling did not occur. With this as the osmium structure, the sign sequence of Worthington and Blaurock is obtained, i.e., $-++--$. This assumption seems to me much less probable than that of highly localized labeling. The sign sequence $+--++$ will therefore be accepted here, and used in what follows.

Finean and Burge (3), and Burge and Draper (4) have found the same sign sequence as Worthington and Blaurock, i.e., the structure negative to mine. Akers and Parsons note that the sequence $--+-$ gives "a positive increase in the intensities of all five reflections" for a certain set of label parameters (reference 1, p. 123); this sequence corresponds to the same density function as does $+--++$, i.e. my structure, but referred to an origin at $l = 0.500$.

Now that the Fourier coefficients for the myelin structure are known, the coefficients for the series describing the heavy atom labeling with $PtCl_4$ and $KMnO_4$ can be inferred from Figs. 4 and 5 of Aker and Parsons. The procedure is the same as that used in constructing Table I. Because all the orders of X-ray reflection show increases as the labeling proceeds, the sign sequence of the myelin structure also applies to the label structures, but the magnitudes of the Fourier coefficients are different for different labels. The electron densities of the OsO_4, $PtCl_4$, and $KMnO_4$ labels are shown, respectively, in Fig. 4 *a*, *b*, and *c*. It is seen that in each case there is a major labeling site at nearly the same place in all three density functions: for OsO_4 at $l = 0.202$, for $PtCl_4$ at $l = 0.220$, and for $KMnO_4$ at $l = 0.210$. This would seem to indicate a chemically active layer in this neighborhood, across which the detailed reactivity varies slightly. The centers of the layers of specific chemical reactivity thus range over a thickness of $(0.220–0.202) \times 171 = 3.08$ A. This is small enough to allow the hypothesis that a single layer of chemically active sites exists to which the heavy atoms attach themselves in geometrically different ways, depending on their structural-chemical properties. It is possible that the smaller peaks in Fig. 4 *a*, *b*, and

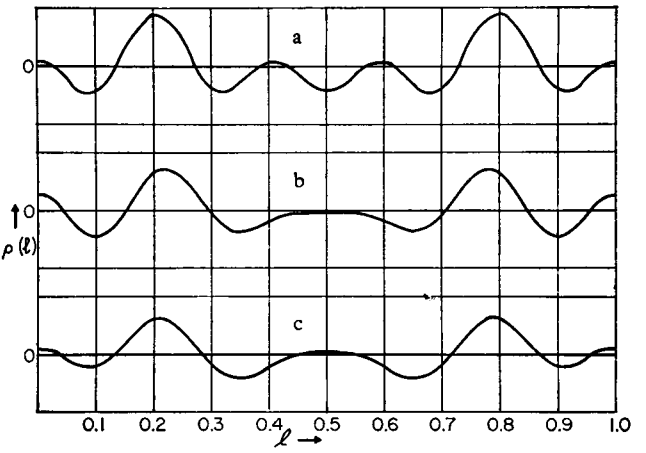

FIGURE 4 Five-term Fourier series for the electron densities of the heavy metal labels on myelin. (*a*) OsO_4, (*b*) $PtCl_4$, (*c*) $KMnO_4$. Coefficients are the differences between the quantities $[hI(h)]^{1/2}$ for the labeled and untreated myelin with the sign sequence $+--++$. (The vertical scale is arbitrary.)

c represent minor labeling sites, but it is also possible that they are "noise" caused by the termination of the Fourier series after only five terms. Future work may decide what their significance may be.

DESCRIPTION OF THE MYELIN STRUCTURE

The image of the myelin structure derived here, and shown in Fig. 3, has a resolution of about 20 A; any detail on a smaller scale cannot be distinguished. There is a high density region centered at $l = 0.225$ with minor density maxima at $l = 0.000$ and $l = 0.500$; these last may not correspond to features of the true structure, but may reflect the effect of cutting off the Fourier series after only five terms, as remarked before. The image in Fig. 3 is compatible with the existence in the myelin single layer of a dense protein lamina of any thickness less than about 15 A centered near $l = 0.225$, or about 38.5 A from one boundary of the layer and 47.0 A from the other. The less dense material between the protein lamina and the boundaries must be mainly lipids, but may contain other substances as well. The single layer is unsymmetrical; the thinner lipid layers of two adjacent single layers are fastened tightly together, back-to-back, to form the double layer. The thicker lipid layers do not stick together so well; the work of Worthington and Blaurock, described in reference 2, shows that sucrose solution can enter at this interface and cause the multilayer to swell. The thinner and thicker lipid layers thus very likely have hydrophobic and hydrophilic outer surfaces, respectively. It is very encouraging to find the single myelin layer to be unsymmetrical, in view of the different transport properties of many membranes in the two opposed directions.

MODEL FOR THE MYELIN STRUCTURE

If it is assumed that the electron density in the lipid portions of the myelin double layer is a constant, and that only the two protein laminae are of greater density than this background, then the values of $|F(h)|$ can be computed from the equation

$$F(h) = f'_0 e^{-A'h^2} \cos 2\pi h l', \tag{4}$$

and compared with those in Table II. The variable parameters f'_0, A', and l' can be found by trial and error in this simple case. The results of these calculations were: $f'_0 = 37.5$, $A' = 0.008$, $l' = 0.232$. Using these in equation 4 gives the numbers in the row of Table II marked "$|F(h)|$ calc." It is seen that they differ from the values of "mean $|F(h)|$ obs" by amounts less than or about equal to $\sigma(|F(h)|)$, except for $h = 3$; they therefore fit the experimental data about as well as these agree among themselves. For this comparison $R = 0.078$, which indicates better agreement than that between any two of the three sets of experimental $|F(h)|$'s. The value of R for the comparison between $|F(h)|$ calc and the $|F(h)|$'s of Fig. 2 of Akers and Parsons is 0.109, the same for Fig. 4 of Akers and Parsons is 0.073, while for Fig. 5 it is 0.101; the average of these is 0.094. Again the agreement between the observed and calculated sets of numbers is better than that between any two observed sets. It would therefore appear that any better fit of the observed data, brought about by using a more elaborate model from which to compute values of $|F(h)|$ calc, would not indicate that model's superiority over the one on which equation 5 is based. No such R for unlabeled myelin is presented in Akers and Parsons. They could not compute one without assuming a detailed model, and this they did not do.

The structure corresponding to this calculation consists of double layers of myelin 171 A thick composed of constant density lipid in which are two centrosymmetrically arranged laminae of protein 6.9 A thick and with centers spaced 79.4 A apart. The distance between the nearest protein laminae in neighboring double layers is $171 - 79.4 = 91.6$ A. These two spacings produce peaks which merge into the peak at $l = 0.5$ in the Patterson function for unlabeled myelin shown in Fig. 3 of Akers and Parsons.

The junctions between the protein lamina and the lipid layers are at about $l' = 0.210$ and $l' = 0.254$; clearly, the heavy atom labeling takes place near the former. These junctions would be expected to have chemical properties different from those of the rest of the myelin layer; apparently, the junction with the thinner, hydrophobic lipid layer is the one that reacts with the heavy atom compounds used as labels by Akers and Parsons. When more quantitative data become available for the higher diffraction maxima, it will be possible to refine the simple model described above by inserting minor fine detail; however, the simple model presented here contains features sufficient to explain satisfactorily the data of Akers and Parsons.

I am happy to mention here the many productive conversations I have had on this subject with Dr. Jacob E. Berger.

I am also grateful to Dr. C. K. Akers and Dr. D. F. Parsons for allowing me to use the original prints from which Figs. 2, 4, and 5 of Akers and Parsons (1) were made.
Dr. G. Kartha kindly carried out the Fourier summations involved in preparing Figs. 1, 3, and 4.

Received for publication 23 April 1971 and in revised form 10 May 1972.

REFERENCES

1. AKERS, C. K., and D. F. PARSONS. 1970. *Biophys. J.* **10**:116.
2. WORTHINGTON, C. R., and A. E. BLAUROCK. 1968. *Nature* (*Lond.*). **216**:87.
3. FINEAN, J. B., and R. E. BURGE. 1963. *J. Mol. Biol.* **7**:672.
4. BURGE, R. E., and J. C. DRAPER. 1965. *Lab. Invest.* **14**:978.